

Supporting Information

Nanofibrous Sunscreen

*BY Byeoungjun Lee†, Hyunwoo Lee†, Chan Park, SungUk Hong, Hyunsuk Jung, Hyonguk Kim, and Seong J. Cho**

[†] These authors equally contributed to this work

[*] Prof. Seong J. Cho
School of Mechanical Engineering
Chungnam National University (CNU), 99 Daehak-Ro, Yuseong-Gu, Daejeon 305-764,
34134 (Republic of Korea)
E-mail: scho@cnu.ac.kr

Byeoung Jun Lee, Hyunwoo Lee, Chan Park, SungUk Hong, Hyunsuk Jung and Hyonguk Kim
School of Mechanical Engineering
Chungnam National University (CNU), 99 Daehak-Ro, Yuseong-Gu, Daejeon 305-764,
34134 (Republic of Korea)

Keywords: UV protection, electrospinning, nanofibrous membrane, nanofibers, cosmetics.

Table S1. Cost estimation of the component for fabrication of nanofibrous sunscreen.

Name	Material	Commercial price (USD)	Cost (USD /cm ²)	Total cost (USD)
Nanofibrous sunscreen	Polyurethane	\$550, 5 kg (Pallethane 2363-80AE, Lubrizol)	0.28	0.48
	Tetrahydrofuran	\$69, 1 L (>99.5%, Sigma Aldrich)	0.01	
	Dimethylformamide	\$50, 1 L (>99.0%, Sigma Aldrich)	0.08	
	Titanium dioxide	\$249, 50 g (Sigma Aldrich)	0.11	
Sunscreen A (Sun mineral cream SPF 50+, Avene, France)			2.4	2.4
Sunscreen B (Mineral Fluid SPF 50+, Avene, France)			2.0	2.0

Table S1 shows the estimation of the component for fabrication of nanofibrous sunscreen.

The fabricated Nanofibrous sunscreen can be used at a cost of about 20% per 1 cm² compared to commercial sunscreens used in the experiment (USD 0.48).

Table S2. Cost estimation of the component for manufacturing PES.

Component	Commercial price (USD)	Usage/device	Cost (USD /device)
Filament	22.3, 1kg (PLA Filament, CUBICON)	58.5g ¹	USD 1.3
HVPS	5.7, 1EA	1EA	USD 5.7
Switch	0.08, 1EA	1EA	USD 0.08
Syringe	4.1, 100EA (KOVAX_SYRINGE 1ml, KOREA)	1EA	USD 0.41
Battery	4.9, 20EA (Bexel, KOREA)	2EA	USD 0.49
Fuse	2.4, 1EA	1EA	USD 2.4
			Total cost: USD 10.38

Table S2 shows the estimation of manufacturing PES costs. The total cost for a device was less than USD 20. The cost of PES has been confirmed to be competitive compared to the commercialized electrospinning device (USD 11,500).

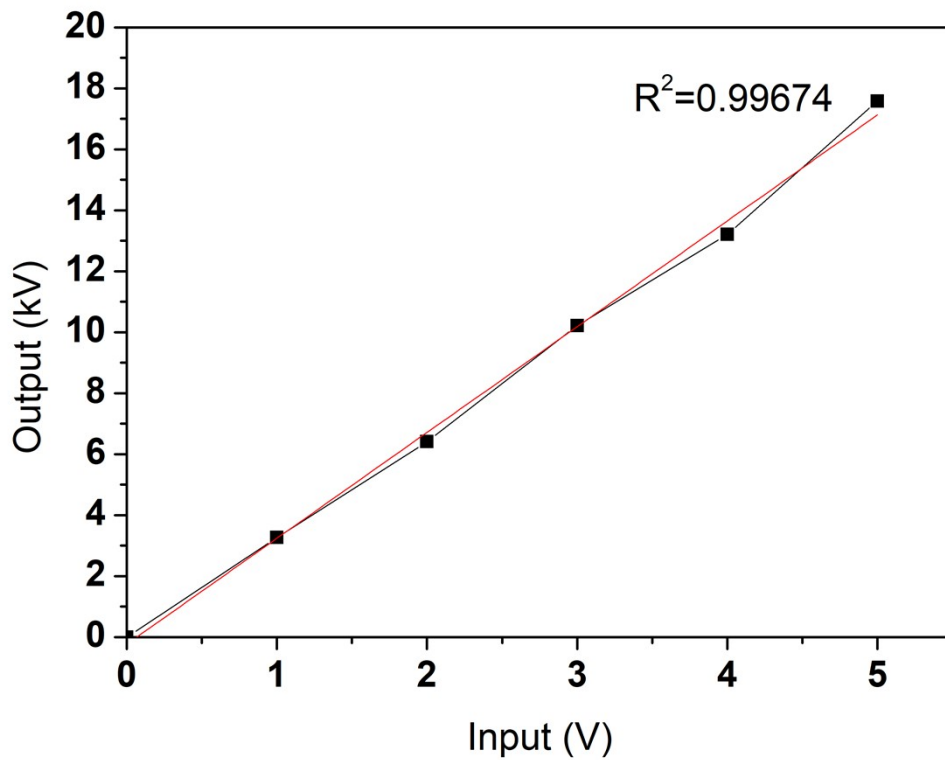


Figure S1. Input-to-output voltage evaluation of PES.

Figure S1 shows the output voltage of PES according to the applied voltage.

A voltage of 1-5 V was provided by the power supply, and the output voltage was amplified from a minimum of 3.3 kV to 17.6 kV through the high voltage amplifier used in the PES.

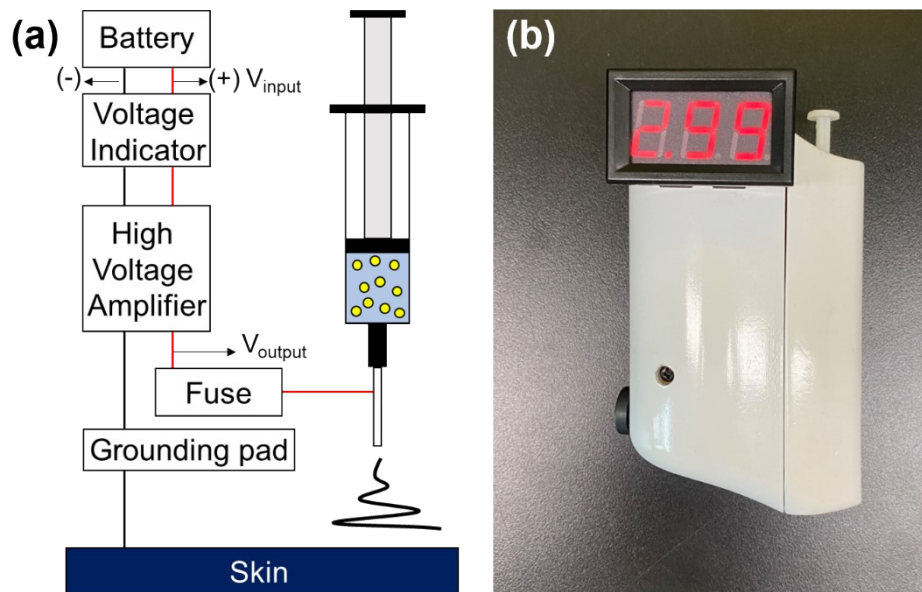


Figure S2. (a) Internal configuration of the PES. (b) Photograph of the PES with voltage indicator.

Figure S2a and b shows internal configuration and photograph the portable electrospinning system with voltage indicator. Voltage indicator display output voltage of portable electrospinning system. Voltage indicator display the input voltage (V_{input}) before the voltage amplifier. The final output voltage (V_{output}) can be calculated as $V_{output}(kV) = 3.473 * V_{input}(V)$ (**Figure S2a**). Users can check the voltage being used when using a portable electrospinning system.

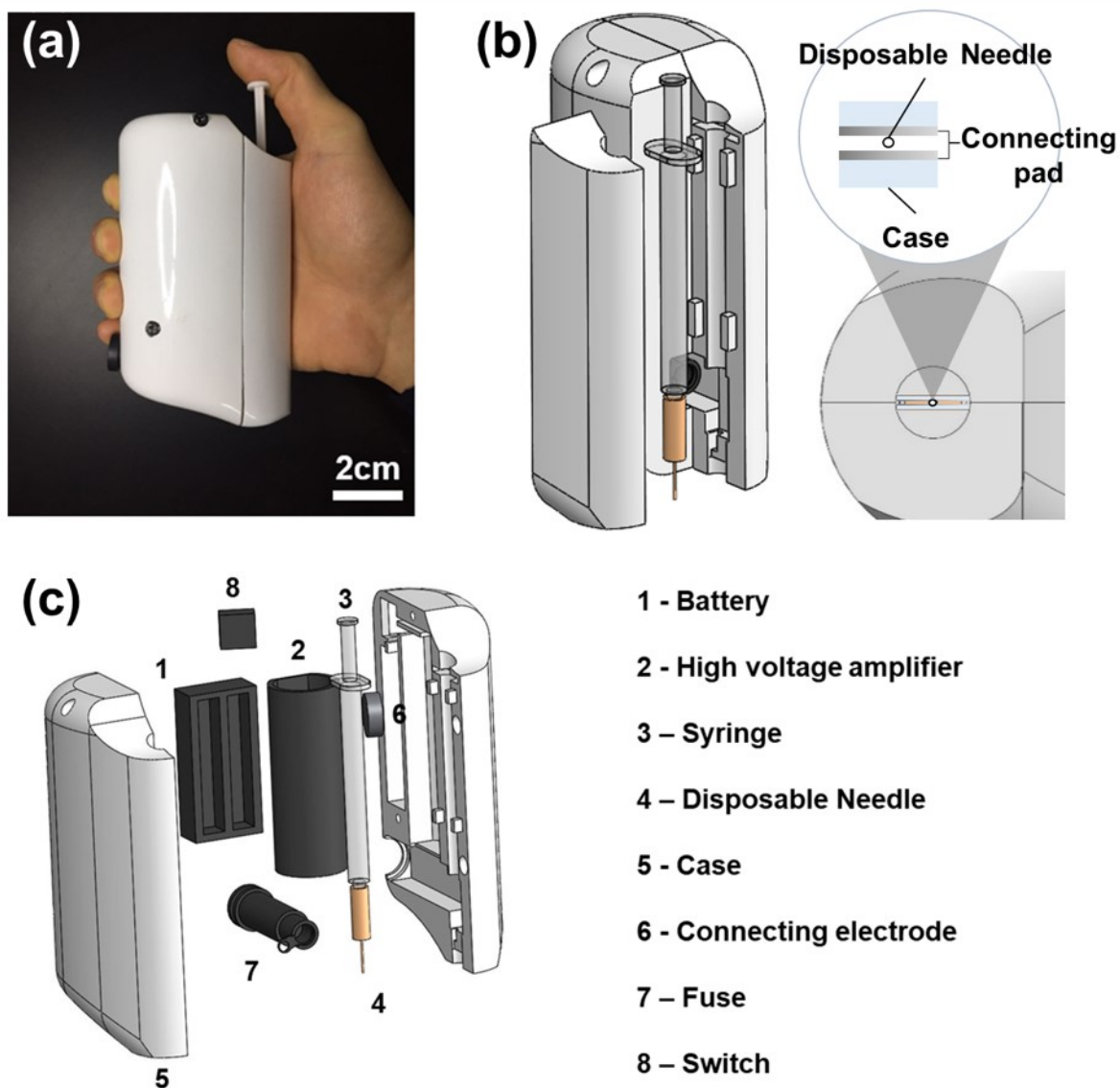


Figure S3. Configuration diagram of a portable electrospinning system. (a) Photograph of the PES held in one hand. (b) PES designed for easy replacement of syringe and disposable needle. (c) Component of a portable electrospinning system.

Figure S3 shows the components of a portable electrospinning system (PES).

The case of PES was made with a 3D printer using PLA material, and commercial products were used for other components. All components except the case are modularized for user convenience and easy replacement. For safety, a fuse circuit is installed to protect against electrical shock. When current between the high voltage amplifier and the syringe tip exceeds 10 mA

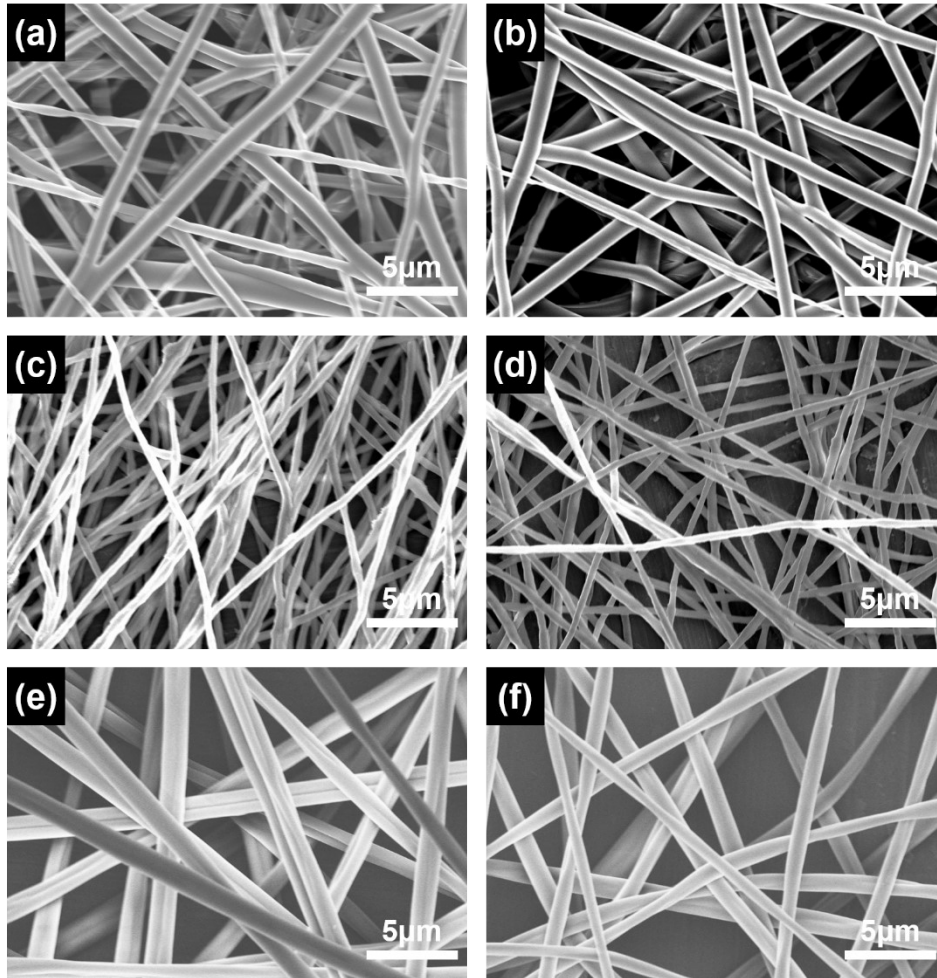


Figure S4. SEM Image of electrospun PU, PEO, PVP nanofibers fabricated by (a,c,e) Conventional electrospinning set-up and (b,d,f) Portable electrospinning system.

Figure S4 (a, c, e) shows electrospun nanofibers fabricated by conventional electrospinning set-up and **Figure S4 (b, d, f)** show electrospun nanofibers fabricated by portable electrospinning system. It was confirmed that there was no difference in the morphology with conventional electrospinning system.

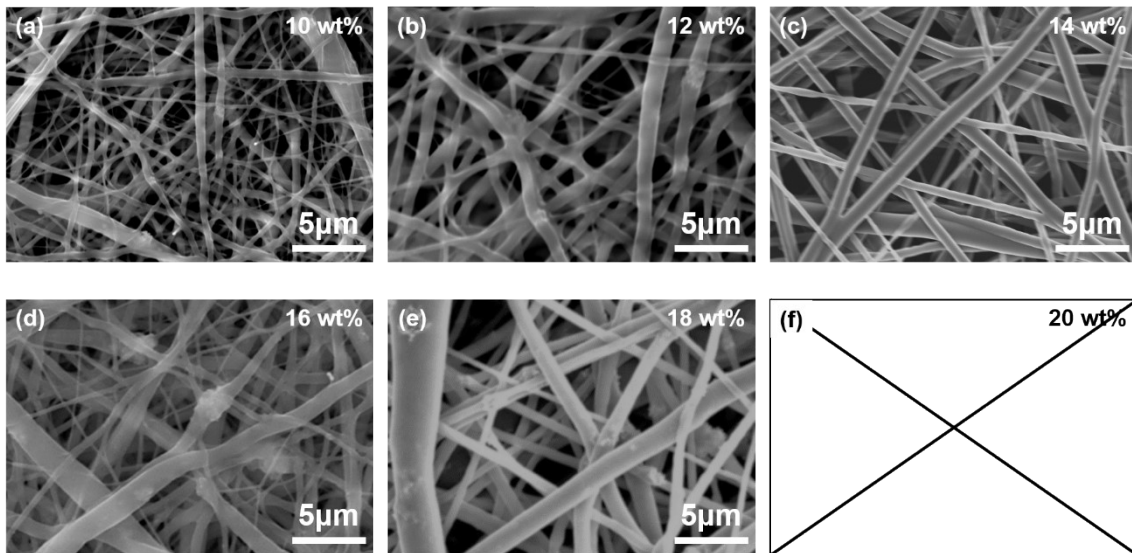


Figure S5. SEM image of electrospun fibers according to concentration of polyurethane solutions ((a) 10 wt%, (b) 12 wt%, (c) 14 wt%, (d) 16 wt%, (e) 18 wt%, and (f) 20 wt%).

Table S3. Characteristics of electrospun fibers according to concentration of polyurethane solutions.

Concentration	10 wt%	12 wt%	14 wt%	16 wt%	18 wt%	20 wt%
Thickness	326.4±148 nm	726.88±185 nm	934.0±150 nm	1106.4±311 nm	1242±265 nm	-
Uniformity	Poor	Fair	Good	Fair	Fair	
Stability	Poor	Fair	Good	Good	Good	-
Beads	Bead generation	Bead generation	No beads	No beads	No beads	-

Figure S5 and Table S3 shows SEM image and characteristic of electrospun fibers according to concentration of polyurethane solutions. as the concentration of the solution decreased, the diameter of the fabricated fibers became thinner. In addition, the formation of the tail cone was unstable, and the jet stability was not good, so the number of beads along the fiber increased (**Figure S5a and b**). On the other hand, as the concentration of the solution increased, the diameter of the fiber became thicker and the tail cone was stably formed. However, the uniformity of the fabricated fibers was not good (**Figure S5d and e**). When the concentration of the solution is 20 wt%, it is difficult to form fibers due to the high viscosity (**Figure S5f**). Therefore, in this study, a 14 wt% solution with a stable tail cone formation, no

beads, and good uniformity was selected as a solution concentration suitable for nanofibrous sunscreen (**Figure S5c**).

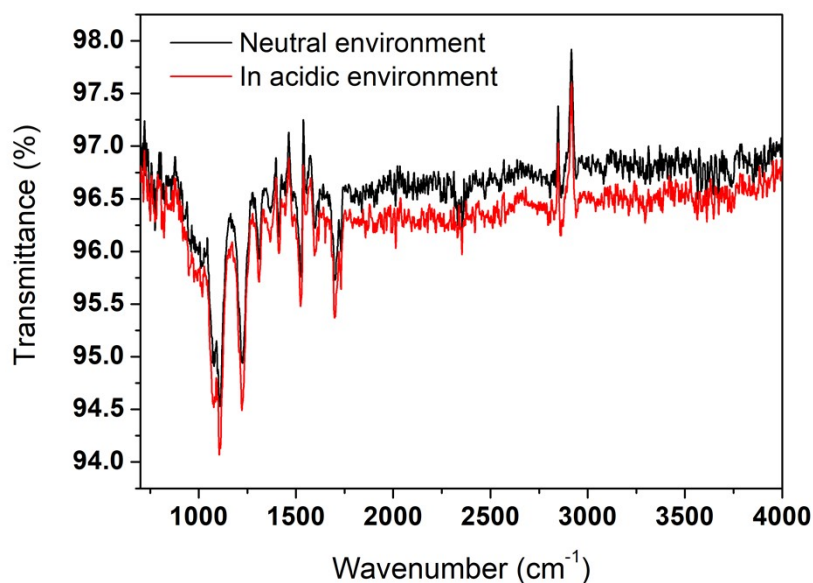


Figure S6. FT-IR spectra of nanofibrous sunscreen in neutral environment and nanofibrous sunscreen exposed to slightly acidic environment.

Figure S6 shows FT-IR spectra of nanofibrous sunscreen. **In Figure S4**, acid-exposed nanofibrous sunscreen and neutral nanofibrous sunscreen showed the same phase graph, and new or lost peaks were not observed. It means that the acidic environment did not affect the chemical bonding structure of nanofibrous sunscreen. Therefore, it can be seen that nanofibrous sunscreen can be applied even in a slightly acidic environment.

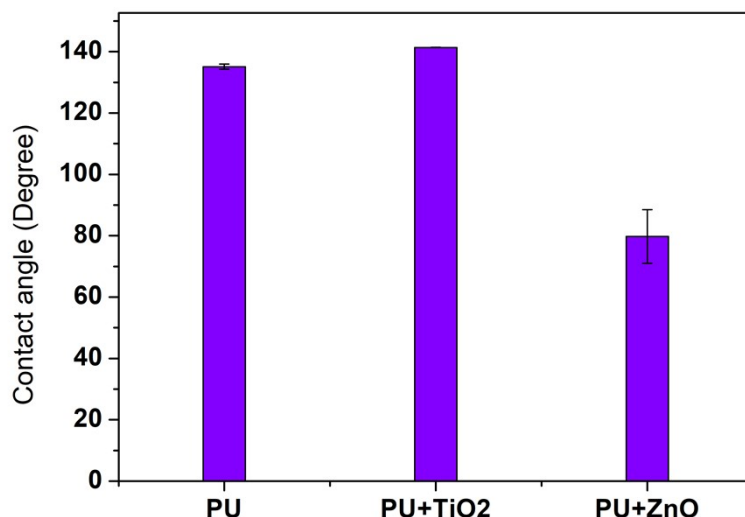


Figure S7. Contact angle of nanofibrous susncreen with different particles.

Figure S7 shows the contact angles of PU, PU + TiO₂, and PU + ZnO membranes. The contact angles of PU and PU + TiO₂ are $135.10^{\circ} \pm 0.85$ and $141.36^{\circ} \pm 0.31$, respectively, and the contact angle of PU + ZnO is $79.5^{\circ} \pm 8.71$. In the case of PU and PU + TiO₂, the membrane surface is hydrophobic, and in the case of PU + ZnO, the membrane surface is hydrophilic. Through this, it was confirmed that the PU + TiO₂ membrane can be used in a wet environment.

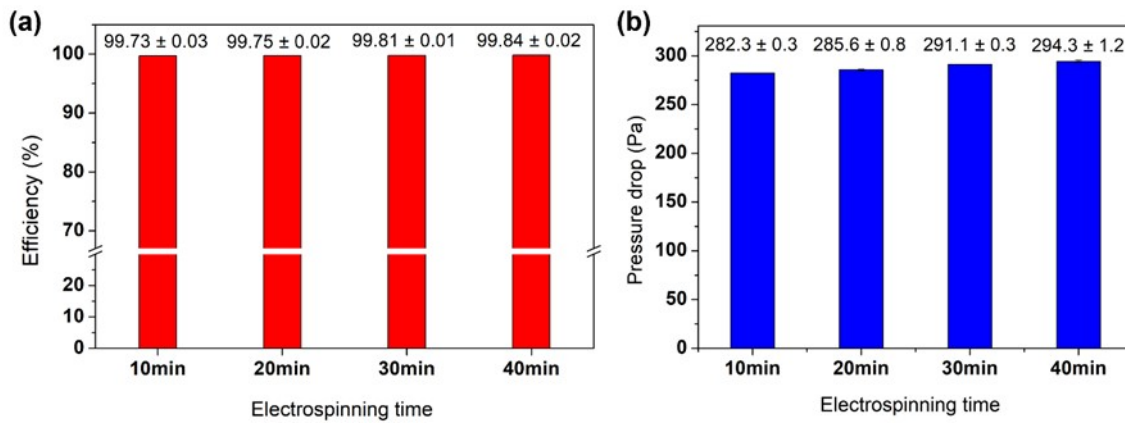


Figure S8. (a) Filtering efficiency and pressure drop of nanofibrous sunscreen according to electrospun time.

Figure S8(a) and S8(b) shows filtering efficiency and pressure drop of nanofibrous sunscreen according to electrospun time. In the case of filtering efficiency, it slightly increased as the electrospinning time increased, showing an efficiency of up to 99.84%. And the pressure drop increased from 282.3 Pa to 394.3 Pa. This is advantageous for filtering particle matter as the electrospinning time increases, but the pressure drop increases and air permeability is not secured. In the case of filtering efficiency and pressure drop, there is a trade-off relationship. Therefore, we decided that 10 min was suitable for spinning in consideration of the manufacturing goal of portable electrospinning device and user convenience.